

## Output Signal Characteristics of a Post-detection EGC Combiner with Two ASK Input Signals in the Presence of Fading and Gaussian Noise

**Đ. V. Bandur, M. V. Bandur**

The Faculty of Technical Sciences, University of Pristina,  
Kneza Milosa str. 7, 38220 Kosovska Mitrovica, Serbia, dbandjur@gmail.com

**M. Č. Stefanović,**

The Faculty of Electronic Engineering, University of Nis,  
Beogradska str. 14, 18000 Nis, Serbia

### Introduction

In this paper we analyze a dual-branch diversity system in order to reduce the impact of fading on an amplitude-shift-keyed (ASK) receiver. An equal-gain combiner (EGC) with post-detection combining and non-coherent demodulation is used. After passing through the fading channel, the input signal is contaminated at the receiver by additive white Gaussian noise (AWGN). Probability density of the input signal amplitude is variable due to impact of fading. We applied Nakagami- $m$  distribution in order to model impact of fading. This distribution is successfully used in modeling land-mobile and indoor-mobile multipath propagation, as well as ionospheric radio links [1].

There is a large number of papers dealing with the performance of non-coherent detection systems over additive white Gaussian noise as well as fading channels, for example in [1] Proakis developed a generic expression for evaluating the bit-error rate for multichannel non-coherent and differentially coherent reception of binary signals over  $L$  independent AWGN channels. Further, in [2] Proakis provided closed-form expressions for average bit error (ABER) of binary orthogonal square-law detected frequency-shift keying (FSK) and binary differential phase-shift keying (DPSK) systems with multi-channel reception over  $L$  independent identically distributed Rayleigh fading channels.

### Non-coherent demodulation in case of no fading impact

The object of our analysis is a receiver with two independent and uncorrelated diversity branches shown in the Fig.1. Each diversity branch performs non-coherent demodulation of the input ASK signal and consists of two elements: a narrowband filter and an envelope detector. The input signals are defined by the following expression

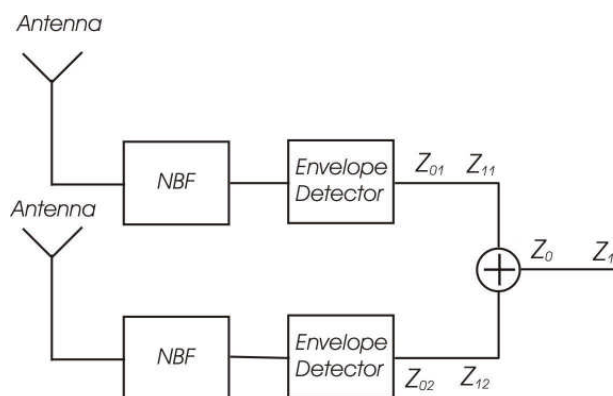


**Fig. 1.** Receiver with two diversity branches and non-coherent demodulation

$$s(t) = \begin{cases} 0, & \text{hypothesis } H_0; \\ A \cos \omega t, & A \geq 0. \text{ hypothesis } H_1. \end{cases} \quad (1)$$

Additionally, input signals are contaminated by AWGN, whose variance passing through a narrowband filter becomes  $\sigma^2$ .

The output signals from the diversity branches  $z_{01}$ ,  $z_{11}$ ,  $z_{02}$  and  $z_{12}$  are combined at the EGC combiner. The first subscript symbol denotes hypothesis, while the second one denotes diversity branch. The probability density functions (PDF) of the signals in diversity branches are given by the following expressions, in case of the hypotheses  $H_0$  and  $H_1$ , respectively [3]

$$p_{z_{01}}(z_{01}) = \frac{z_{01}}{\sigma_1^2} e^{-\frac{z_{01}^2}{2\sigma_1^2}}, \quad z \geq 0; \quad (3)$$

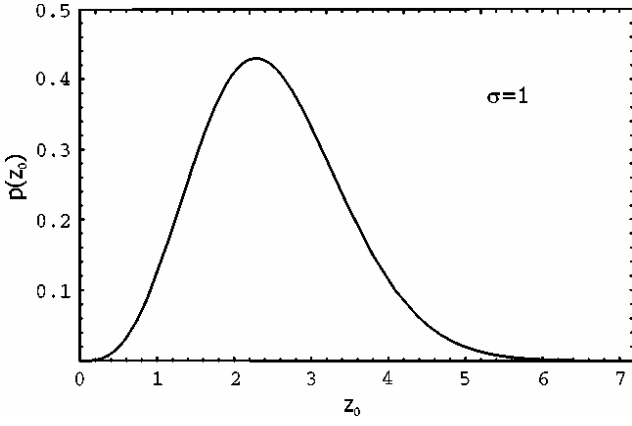


Fig. 2. PDF of the signal  $z_0$  at the EGC combiner output

$$p_{z_{02}}(z_{02}) = \frac{z_{02}}{\sigma_2^2} e^{-\frac{z_{02}^2}{2\sigma_2^2}}, \quad z \geq 0; \quad (4)$$

$$p_{z_{11}}(z_{11}) = \frac{z_{11}}{\sigma_1^2} e^{-\frac{z_{11}^2 + A_1^2}{2\sigma_1^2}} I_0\left(\frac{z_{11}A_1}{\sigma_1^2}\right), \quad z \geq 0; \quad (5)$$

$$p_{z_{12}}(z_{12}) = \frac{z_{12}}{\sigma_2^2} e^{-\frac{z_{12}^2 + A_2^2}{2\sigma_2^2}} I_0\left(\frac{z_{12}A_2}{\sigma_2^2}\right), \quad z \geq 0. \quad (6)$$

Let  $z_0$  and  $z_1$  be the EGC combiner output signals, defined as  $z_0 = z_{01} + z_{02}$  and  $z_1 = z_{11} + z_{12}$ . The PDF of the  $z_0$  and  $z_1$  in case of the hypotheses  $H_0$  and  $H_1$ , is given by [4], respectively

$$p_{z_0}(z_0) = \int_0^{z_0} p_{z_{01}}(z_0 - z_{02}) p_{z_{02}}(z_{02}) dz_{02}, \quad (7)$$

$$p_{z_1}(z_1) = \int_0^{z_1} p_{z_{11}}(z_1 - z_{12}) p_{z_{12}}(z_{12}) dz_{12}. \quad (8)$$

Substitutions of (3) and (4) in (7), as well as (5) and (6) in (8), give the following expressions

$$p_{z_0}(z_0) = \int_0^{z_0} \frac{z_0 - z_{02}}{\sigma_1^2} e^{-\frac{(z_0 - z_{02})^2 + A_1^2}{2\sigma_1^2}} \frac{z_{02}}{\sigma_2^2} e^{-\frac{z_{02}^2}{2\sigma_2^2}} dz_{02}, \quad (9)$$

$$p_{z_1}(z_1) = \int_0^{z_1} \frac{z_1 - z_{12}}{\sigma_1^2} e^{-\frac{(z_1 - z_{12})^2 + A_1^2}{2\sigma_1^2}} I_0\left(\frac{(z_1 - z_{12})A_1}{\sigma_1^2}\right) \times \frac{z_{12}}{\sigma_2^2} e^{-\frac{z_{12}^2 + A_2^2}{2\sigma_2^2}} I_0\left(\frac{z_{12}A_2}{\sigma_2^2}\right) dz_{12}. \quad (10)$$

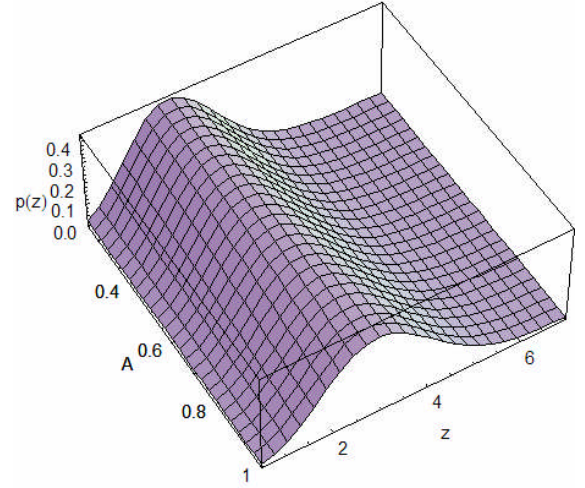


Fig. 3. 2-D PDF of the signal  $z_1$  at the EGC combiner output

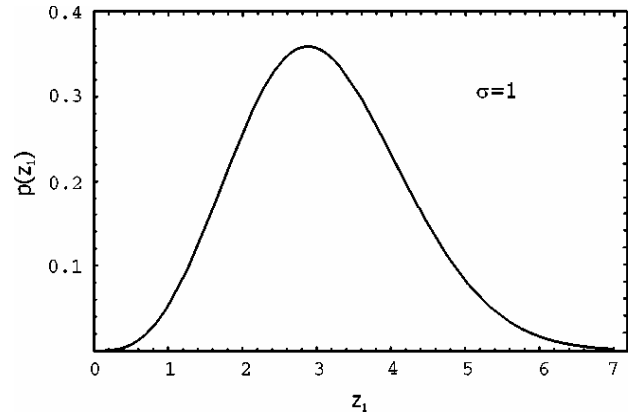


Fig. 4. A front-end intersection of the Fig. 3

The Fig. 2. is a graphical interpretation of (9), while the Fig. 3 and Fig. 4 are two-dimensional graphical interpretation of (10), i.e. the PDF of the signal  $z_1$  at the EGC combiner output, and its front-end intersection, respectively.

### Non-coherent demodulation in the presence of fading

Fluctuation of the transmitted signal envelope is a channel fading consequence. In this paper, fading is statistically modeled by Nakagami- $m$  distribution [1]:

$$p(A) = \frac{2}{\Gamma(m)} \left(\frac{m}{\Omega}\right)^m A^{2m-1} e^{-\frac{m}{\Omega}A^2}, \quad A \geq 0, \quad m \geq \frac{1}{2}; \quad (11)$$

where  $\Omega$  – rms (root-mean-square) of received envelope;  $m$  – fading severity index, and  $\Gamma(\cdot)$  – denotes the Gamma function.

The PDF of the EGC output signal, i.e.  $z_1$ , is defined by (8). However, by taking into account the impact

of Nakagami- $m$  distributed fading, the PDF of the first diversity branch, i.e.  $p_{z_{11}}(z_{11})$  can be expressed as

$$p_{z_{11}}(z_{11}) = \int_0^{\infty} \frac{z_{11}}{\sigma_1^2} e^{-\frac{z_{11}^2 + A_1^2}{2\sigma_1^2}} I_0\left(\frac{z_{11}A_1}{\sigma_1^2}\right) p(A_1) dA_1, \quad z \geq 0; \quad (12)$$

$$p_{z_{11}}(z_1 - z_{12}) = \int_0^{\infty} \frac{z_1 - z_{12}}{\sigma_1^2} e^{-\frac{(z_1 - z_{12})^2 + A_1^2}{2\sigma_1^2}} \times I_0\left(\frac{(z_1 - z_{12})A_1}{\sigma_1^2}\right) \frac{2}{\Gamma(m_1)} \left(\frac{m_1}{\Omega_1}\right)^{m_1} A_1^{2m_1-1} e^{-\frac{m_1 A_1^2}{\Omega_1}} dA_1; \quad (14)$$

$$p_{z_{11}}(z_1 - z_{12}) = \frac{z_1 - z_{12}}{\sigma_1^2} e^{-\frac{(z_1 - z_{12})^2}{2\sigma_1^2}} \frac{2}{\Gamma(m_1)} \left(\frac{m_1}{\Omega_1}\right)^{m_1} \times \int_0^{\infty} A_1^{2m_1-1} e^{-\frac{A_1^2}{2\sigma_1^2}} e^{-\frac{m_1 A_1^2}{\Omega_1}} I_0\left(\frac{(z_1 - z_{12})A_1}{\sigma_1^2}\right) dA_1; \quad (15)$$

$$p_{z_{11}}(z_1 - z_{12}) = \sum_{k=0}^{\infty} \frac{(z_1 - z_{12})^{2k+1}}{4^k k! \sigma_1} e^{-\frac{(z_1 - z_{12})^2}{2\sigma_1^2}} \times \frac{\Gamma(m_1 + k)}{\Gamma(m_1)\Gamma(k+1)} \left(\frac{m_1}{\Omega_1}\right)^{m_1} \left(\frac{2\sigma_1^2 \Omega_1}{2\sigma_1^2 m_1 + \Omega_1}\right)^{m_1+k}; \quad (16)$$

where  $I_0(z) = \sum_{k=0}^{\infty} \frac{z^{2k}}{2^{2k} k! \Gamma(k+1)}$  [5], and the appropriate

graphical interpretation is given in the Fig.5. On the same way can be derived the PDF of the second EGC diversity branch, i.e.  $p_{z_{12}}(z_{12})$ .

$$p_{z_{12}}(z_{12}) = \int_0^{\infty} \frac{z_{12}}{\sigma_2^2} e^{-\frac{z_{12}^2 + A_2^2}{2\sigma_2^2}} I_0\left(\frac{z_{12}A_2}{\sigma_2^2}\right) p(A_2) dA_2, \quad z \geq 0; \quad (17)$$

$$p_{z_{12}}(z_{12}) = \sum_{j=0}^{\infty} \frac{z_{12}^{2j+1}}{4^j j! \sigma_2^{4j+2}} e^{-\frac{z_{12}^2}{2\sigma_2^2}} \frac{\Gamma(m_2 + j)}{\Gamma(m_2)\Gamma(j+1)} \times \left(\frac{m_2}{\Omega_2}\right)^{m_2} \left(\frac{2\sigma_2^2 \Omega_2}{2\sigma_2^2 m_2 + \Omega_2}\right)^{m_2+j}. \quad (18)$$

Hence, by substituting (16) and (18) in (8), and after some straight forward mathematical manipulations, the final expression for the PDF of the EGC output signal can be derived as in (19), and plotted in Fig.6.

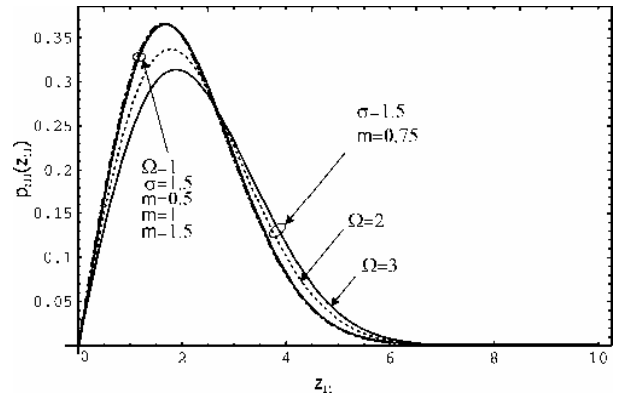


Fig. 5. PDF of the  $z_{11}$ , i.e.  $z_{12}$

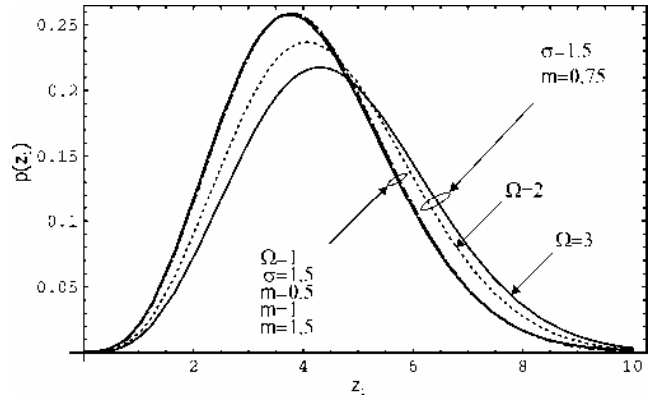


Fig. 6. PDF of the signal  $z_1$  at the EGC combiner output

$$p_{z_1}(z_1) = \sum_{k=0}^{\infty} \sum_{j=0}^{\infty} \frac{\Gamma(m_1 + k)\Gamma(m_2 + j)}{4^{k+j} k! j! \Gamma(m_1)\Gamma(m_2)\Gamma(k+1)\Gamma(j+1)} \times \frac{1}{\sigma_1^{4k+2} \sigma_2^{4j+2}} \left(\frac{m_1}{\Omega_1}\right)^{m_1} \left(\frac{m_2}{\Omega_2}\right)^{m_2} \times \left(\frac{2\sigma_1^2 \Omega_1}{2\sigma_1^2 m_1 + \Omega_1}\right)^{m_1+k} \left(\frac{2\sigma_2^2 \Omega_2}{2\sigma_2^2 m_2 + \Omega_2}\right)^{m_2+j} \times \int_0^{z_1} (z_1 - z_{12})^{2k+1} z_{12}^{2j+1} e^{-\frac{(z_1 - z_{12})^2}{2\sigma_1^2} - \frac{z_{12}^2}{2\sigma_2^2}} dz_{12}. \quad (19)$$

Capitalizing on this, many other important statistical parameters can be calculated as well. For example, by definition the cumulative density function and moments of the EGC output signal can be expressed by substituting (19) in the following equations, respectively

$$P(\gamma) = \int_0^{\gamma} p_{z_1}(z_1) dz_1; \quad (20)$$

$$\mu(r) = \int_0^{\infty} z_1^r p_{z_1}(z_1) dz_1. \quad (21)$$

## Numerical Results Discussion

For the convenience of the results presentation it is assumed that the fading parameters of the both diversity branches are identical. The PDF expressions (16) and (18) are very fast converging. Numerical results show that the first few infinite series terms are enough for obtaining the targeted accuracy. However, due to very complicated nature of expression (19), it is very difficult, if not impossible, to derive a closed-form solution for convolution integral in (19). On the other hand, it can be evaluated via numerical integration using any of the well-known mathematical software packages. The shapes of the PDF curves, Fig. 5 and Fig. 6, almost exclusively depend on the average fading power  $\Omega$ , while fading severity index  $m$  very slightly affects probability distribution of the EGC output signal.

## Conclusion

In this paper we presented an infinite series expression for the PDF of the signal at the dual branch EGC combiner output in a fading environment with the presence of white

Gaussian noise. Capitalizing on this, the cumulative distribution function, average bit error rate, outage probability as well as the second order statistics and other criteria needed for the system performance evaluation can be easily calculated.

## References

1. **Proakis J. G.** On the probabilities of error for multichannel reception of binary signals // IEEE Trans. Commun. Technol. – Feb. 1968. – Vol. COM-16. – P. 68–71.
2. **Proakis J. G.** Digital Communications. 3<sup>rd</sup> ed. – New York: McGraw-Hill, 1995. – P. 774–775.
3. **Mihajlo C Stefanovic.** Signal detection in white and colored Gaussian noise // Univeristy of Nis. – 1999. – P. 436–437.
4. **Khairi Ashour Hamdi.** Exact probability of BPSK communication links subjected to asynchronous interference in Rayleigh fading environment // IEEE Transactions on Communications. – October 2002. – Vol. 50, No.10. – P. 1577–1579.
5. **Abramowitz M., and Stegun I. A. (Eds.)** Modified Bessel Functions  $I$  and  $K$ . – §9.6 in Handbook of Mathematical Functions with Formulas, Graphs, and Mathematical Tables. – 9th printing, New York: Dover, 1972. – P. 374–377.

Submitted for publication 2007 10 15

**Đ. V. Bandur, M. V. Bandur, M. C. Stefanović.** Output Signal Characteristics of a Post-detection EGC Combiner With Two ASK Input Signals in Presence of Fading and Gaussian Noise // *Electronics and Electrical Engineering*. – Kaunas: Technologija, 2008. – No. 2(82). – P. 41–44.

The output signal of a noncoherent dual branch receiver with EGC combiner in presence of Nakagami fading and additive white Gaussian noise will be considered in this paper. The PDF of the receiver branch signal as well as the PDF of the EGC combiner output signal will be calculated and displayed in this paper. The mentioned probability density functions will provide an necessary assumption for determination of the other important receiver characteristics and parameters. Ill. 6, bibl. 5 (in English; summaries in English, Russian and Lithuanian).

**Д. В. Бандур, М. В. Бандур, М. С. Стефанович.** Характеристики выходного сигнала смесителей EGC с двумя сигналами входа в присутствии Гауссовского шума и ослабления // *Электроника и электротехника*. – Каунас: Технология, 2008. – № 2(82). – С. 41–44.

Сигнал продукции непоследовательного двойного приемника ветви с объединителем EGC в присутствии исчезновения Nakagami и совокупного белого Гауссовского шума будут рассматривать в этой бумаге. PDF сигнала ветви приемника так же как PDF сигнала продукции объединителя EGC будет рассчитан и показан в этой бумаге. Упомянутые функции плотности вероятности обеспечат необходимое предположение для определения других важных особенностей приемника и параметров. Ил 6, библи. 5 (на английском языке; рефераты на английском, русском и литовском яз.).

**Đ. V. Bandur, M. V. Bandur, M. C. Stefanović.** EGC maišytuvo su dviem ASK įėjimo signalais išėjimo signalo charakteristikos, esant slopinimui ir Gauso triukšmui // *Elektronika ir elektrotechnika*. – Kaunas: Technologija, 2008. – Nr. 2(82). P. 41–44.

Nagrinėjamas nekoherentinio dviejų šakų imtuvo su EGC maišytuvu išėjimo signalas, esant Nakagami pobūdžio slopinimui ir adityvaus pobūdžio baltajam Gauso triukšmui. Apskaičiuota ir pateikta imtuvo šakos signalo PDF ir EGC maišytuvo išėjimo signalo PDF. Pateiktos tikimybės tankio funkcijos užtikrina būtinas prielaidas, reikalingas norint nustatyti kitas svarbias imtuvo charakteristikas ir parametrus. Il. 6, bibl. 5 (anglų kalba; santraukos anglų, rusų ir lietuvių k.).

DOI: 10.5755/j02.eie.11052